

1 **Effect of landfill leachate ageing on ultrafiltration**

2 **performance and membrane fouling behaviour**

3 Sergio Collado^a, Daniel Núñez^a, Paula Oulego^a, Francisco A. Riera^a, Mario Díaz^{a*}

4 ^a*Department of Chemical and Environmental Engineering*

5 *University of Oviedo c/ Julian Claveria s/n, E-33071, Oviedo, Spain*

6 ^(*) *phone: (+34) 985 10 34 41, fax: (+34) 985 10 34 34 email: mariodiaz@uniovi.es*

7 **Abstract:**

8 In this study, the effect of ageing on the performance and fouling mechanisms in the
9 ultrafiltration of landfill leachates using titania-zirconia (ZrO₂-TiO₂) tubular membrane
10 was thoroughly studied. Results revealed that the maturation of the leachate has a positive
11 effect on its ultrafiltration, with a twofold higher final permeability compared with the
12 young one. This is the result of the higher organic load, particularly that corresponding to
13 proteins and carbohydrates, of the young leachate.

14 Resistance-in-series analysis demonstrated that the loss of permeability was mainly due
15 to reversible fouling, caused by cake filtration. Either irrecoverable or irreversible fouling
16 were scarce and not conditioned by the stage of maturation of the leachate. Chemical
17 oxygen demand (COD) rejection for the mature leachate varied with volume
18 concentration ratio (VCR) showing an approximately sigmoidal shape, from an initial
19 value of 18.5% to a final one of 49.6%, with the faster increase at VCR ranging from 1.2
20 to 1.7, due to the permeation of fatty acids by the ultrafiltration (UF) membrane. On the
21 other hand, COD rejection remained approximately constant at 48% during the
22 ultrafiltration of the young leachate, which can be attributed to the presence of higher
23 molecular weight compounds in its composition.

24 **Keywords**

25 Landfill leachate; Wastewater management; Ageing; Ultrafiltration; Fouling modelling

28 **1. Introduction**

29 The increasing solid waste landfilling has led to one of the major environmental
30 challenges of today: the efficient management of the leachates generated. These
31 aqueous wastes, which can be defined as the liquid that passes through a landfill and has
32 extracted dissolved and suspended matter from it, are considered a significant threat to
33 surface water, groundwater and soil [1]. Many factors have been reported that influence
34 leachate composition, such as the age of the landfill, the local climate or season, the
35 depth of the waste in the landfill and, mainly, the composition of the waste material [2–
36 4]. This fact makes leachate matrices significantly complex and variable [5], which in
37 turns means that the improvement and/ or development of a generalized treatment
38 method for any leachate to meet the relevant quality standards is not possible [6]. In
39 fact, leachate treatments are based on process schemes which generally comprise some
40 combination of biological, physical and/or chemical treatment [7–10]. Biological
41 treatments are used for removing the biodegradable organic matter content in the
42 leachate; while chemical and physical treatments such as flotation, coagulation-
43 flocculation, precipitation, adsorption or air stripping are employed as pre-treatments in
44 order to improve the efficiency of a subsequent treatment, or when a biological
45 oxidation process is hampered by the presence of bio-refractory materials, like non-
46 biodegradable (humic and fulvic acids) and/or undesirable compounds (heavy metals,
47 AOXs, PCBs...). Besides, these treatments can also be employed as post-treatments
48 after a biological one with the aim of ensuring final polishing level by removing toxic
49 metals and organic compounds [6,10]. Advanced oxidation processes (AOPs), such as
50 ozonation (alone or in combination with UV) and UV/TiO₂ photocatalysis, which are a
51 particular case of chemical treatment, can also be used as post-treatments after
52 biodegradation processes for removing recalcitrant compounds [6]. In addition to the
53 conventional treatments, physical treatments based on membrane technology have
54 emerged as viable alternatives to reach the level of purification needed to fully reduce
55 the negative impact of landfill leachates on the environment. Either as a main step in a
56 landfill leachate treatment chain or as a single treatment step, the use of membrane
57 technologies has shown to be an indispensable means of achieving a high degree of
58 purification of this stream [10]. Among the various membrane technologies,
59 ultrafiltration (UF) is used in separation and purification because of its high efficiency
60 and lower energy consumption, thus reducing treatment costs [11].

61 UF is effective in eliminating macromolecules and particles; around 50% of organic
62 matter can be separated from the leachate [12,13]. Although a study reported UF as a
63 sufficient treatment to ensure the discharge standards for a leachate [13], this technique
64 is not individually used, but in combination with others. Thus, UF can serve as a pre-
65 treatment prior to reverse osmosis [14–17], nanofiltration [15], evaporation [18] or
66 Fenton oxidation [19]; and as a post-treatment for biologically active carbon [20],
67 adsorption [12,15,21], coagulation [15], lime addition [22], nanofiltration (for the
68 concentrate generated) [23], air stripping and coagulation [24] or Fenton reaction and
69 neutralization [25]. Particularly, this technique can also be effective as a pre-treatment
70 for biological degradation of landfill leachate, since it helps reducing the content in
71 humic acids, which can compromise the efficiency of the biological treatment.

72 At this point, it should be noted that, to the best of our knowledge, the effect of the
73 landfill leachate age on the membrane performance has not been studied yet. This is
74 surprising because, although there are many factors affecting the composition of such
75 leachates, this varies greatly depending on the age of the landfill and, thus, the degree of
76 solid waste stabilization [26]. In fact, two types of leachates have been defined
77 according to landfill age: young and mature. Young leachates are those which come
78 from landfills less than 1 year old, with chemical oxygen demand (COD) values above
79 15 g/L and the ratio between the biodegradable matter (as biological oxygen demand
80 (BOD₅)) and the total organic one (as COD) higher than 0.5. On the other hand, mature
81 leachates are those from facilities which are more than 5 years old (maturation phase)
82 with COD values below 3 g/L and mainly composed of a refractory mixture of humic
83 substances. Their BOD₅ to COD ratio is lower than 0.1 [7,10].

84 It should be noted that the results of ultrafiltration reported in the bibliography for
85 leachates, either for the individual operation or coupled with other processes, are highly
86 subjected to the age of the specific leachate selected for each experimentation, thus
87 making the comparison between the findings of the different studies difficult.

88 In view of these considerations, the aim of this work was to study, for the first time
89 ever, the effect of the landfill leachate age on the quality of the effluent treated by UF as
90 a pre-treatment prior to a biological process, as well as modelling the fouling
91 mechanism of the membrane.

92 **2. Experimental**

93 2.1. Landfill leachates

94 All the leachates used in this study were obtained from the sanitary landfill site La
 95 Zoreda and provided by COGERSA (Asturias, Spain). Two different leachates were
 96 employed during the experimentation: mature (M) and young (Y). The young leachate
 97 was obtained from a new area of the landfill which is in expansion. Regarding the
 98 mature leachate, it comes from an area of the landfill where wastes has not been
 99 deposited since 2010.

100 A description of the main physicochemical characteristics of the different leachates can
 101 be found in Table 1. Higher colour value in young leachate has already been reported
 102 [27], and can be explained by higher total organic carbon (TOC) and suspended solid
 103 concentrations. Leachates were pre-filtered with a metal mesh filter of 250 µm of pore
 104 size and 200 mm of diameter (Cisa, Spain) to remove coarse particles. Samples were
 105 stored at 5°C before being used.

Parameter	Type of landfill leachate	
	Old leachate	Young leachate
pH	8.2 ± 0.4 [7.8]	8.8 ± 0.2 [8.7]
COD (mg O ₂ /L)	4005 ± 592 [3960]	7559 ± 2414 [5548]
TOC (mg/L)	n/a [641]	n/a [1784]
Humic acid (mg/L)	n/a [137]	n/a [90]
BOD ₅ (mg O ₂ /L)	559 ± 280 [372]	2435 ± 974 [3077]
Colour Number	n/a [1.322]	n/a [1.573]
Suspended solids (mg/L)	29 ± 24 [30]	92 ± 65 [100]
NH ₄ ⁺ (mg/L)	2200 ± 368 [2323]	2959 ± 427 [3247]
Cl ⁻ (mg/L)	n/a ⁽¹⁾	3329 ± 1182 [3136]
NO ₃ ⁻ (mg/L)	5 ± 1 [4]	3 ± 2 [2]
NO ₂ ⁻ (mg/L)	1.0 ± 0.5 [1]	2 ± 1 [2]
Alkalinity (mg CaCO ₃ /L)	212 ± 28 [221]	258 ± 36 [281]
Conductivity (µS/cm)	21089 ± 4557 [23800]	25737 ± 3323 [19990]

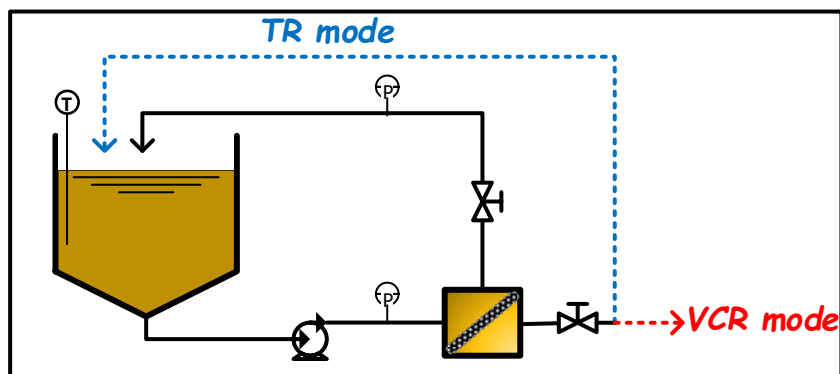
106 ⁽¹⁾n/a= not available

107 **Table 1.** Main characteristics of the mature and young leachates (average values from
 108 2008 to 2018) and values determined in this study (in brackets).

109 2.2. Experimental setup

110 A scheme of the experimental set up is shown in Figure 1. All the ultrafiltration
 111 experiments were conducted using a locally house made and assembled system (Figure
 112 1). This system consisted of a glass vessel of 3 L, where the corresponding leachate was

113 stored and pumped towards the ultrafiltration module using a Masterflex I/P 7591-55
 114 (Cole-Parmer, USA) peristaltic pump attached to an Easyload Masterflex I/P 77601-10
 115 (Cole-Parmer, USA) pump head. Ultrafiltration cell was composed by a tubular ZrO₂-
 116 TiO₂ membrane (600 × 6mm) (TAMI Industries) with an area of 1.14 10⁻² m² and a
 117 molecular weight cut-off (MWCO) of 150 kDa. Ceramic membranes are more resistant
 118 to mechanical, chemical, thermal or biological stresses than polymeric membranes, and
 119 they have been already implemented for wastewater treatment [28]. Also, the use of
 120 ZrO₂-TiO₂ in form of particles [29] or membrane additives [30] has been reported to be
 121 efficient in reducing the fouling caused by humic acid. As for pore size, membrane
 122 MWCO was selected in order to minimize humic acid-caused fouling. In this sense, Yan
 123 et al. [31] have reported that, when ultrafiltrating humic acids, maximum fluxes can be
 124 obtained using membranes within a MWCO range between 100 and 300 kDa. Pressure
 125 gauges and valves were placed in the flow line before and after the ultrafiltration
 126 module in order to measure and set the value of the transmembrane pressure (TMP). All
 127 experiments were carried out at a flow rate of 5.4 L/min and cross flow velocity of 3.2
 128 m/s over the membrane. In order to select the temperature of work, a previous study of
 129 ultrafiltration performance at temperatures from 50°C to 70°C was performed. Lower
 130 fouling rates and higher fluxes were obtained when higher temperatures were used, thus
 131 all experiments were carried out at a steady temperature of 70°C. The permeate flux was
 132 determined by weighing of permeate under a TMP of 1.6 bar. Temperature was kept at
 133 the desired value using a water bath.



134
 135 **Figure 1.** Experimental setup scheme.

136 Two different kinds of experiments were carried out using this experimental setup (see
 137 Figure 1): i) Total recycle (TR) mode and ii) volume concentration ratio (VCR) mode.
 138 The first one is necessary in order to determine the evolution of membrane fouling with

139 time, while the second one is needed to evaluate the effect of concentration on the
140 permeate flux and fouling resistances.

141 Regarding TR mode experiment, retentate and permeate were both completely
142 recirculated to the supply tank and permeate flux was periodically measured until
143 achieving a constant value. Afterwards, membrane was washed with distilled water until
144 the permeate flux did not change with time, and then cleaned at 70°C with 0.5%
145 aqueous solution of basic detergent (Divos 124 VM5 provided by Diversey) until the
146 final flux was higher than 90% of the initial permeate flux [32].

147 In the case of the VCR mode experiment, retentate was also continuously recirculated to
148 the supply tank, but permeate was discarded. Samples of permeate were periodically
149 withdrawn to measure COD, TOC, colour number (CN) and humic acid retentions, as
150 well as permeate fluxes. Leachate filtration was maintained up to a final VCR of 3.
151 Afterwards, the UF membrane was washed and cleaned in the same way than that used
152 in the TR mode test.

153 Both TR and VCR mode experiments were performed at least in duplicate, and in all
154 cases the experimental error was below 5%.

155 2.3. Fouling modelling

156 In order to define the fouling during the ultrafiltration of both leachates in terms of
157 permeability recovery, the next equation was employed (eq. 1):

$$158 \quad J = \frac{TMP}{\mu R_T} = \frac{TMP}{\mu(R_M + R_{rev.} + R_{irrev.} + R_{irrecov.})} \quad (1)$$

159 Where J is the permeate flux ($\text{m}\cdot\text{s}^{-1}$), TMP is the transmembrane pressure ($\text{kg}\cdot\text{m}^{-1}\cdot\text{s}^{-2}$) μ
160 is the dynamic viscosity ($\text{kg}\cdot\text{m}\cdot\text{s}^{-1}$), R_T is the total fouling resistance, R_M is the intrinsic
161 membrane resistance and $R_{rev.}$, $R_{irrev.}$ and $R_{irrecov.}$ are the reversible, irreversible and
162 irrecoverable fouling resistances, respectively (all resistances in m^{-1}). In a practical way,
163 reversible fouling is removed by physical cleaning, irreversible fouling is eliminated by
164 chemical cleaning and irrecoverable fouling refers to those foulants that cannot be
165 removed by any cleaning step [33]. By measuring the initial tap water flux through the
166 membrane (J_0), and the permeate fluxes achieved at the end of the ultrafiltration (J_S)
167 and after the physical (rinsing with distilled water) (J_{pc}) and chemical (J_{cc}) cleanings,

168 the values of each resistance can be calculated according to the methodology included
169 in the Appendix [34].

170 In addition to this resistance-in-series model based on permeability recovery, fouling
171 evolution was also modelled by the Hermia's model [35] with the aim of obtaining an
172 in-depth knowledge of the fouling mechanisms involved (eq. 2).

$$173 \quad \frac{dJ}{dt} = -K \cdot (J - J_0) \cdot J^{2-n} \quad (2)$$

174 Where K is a constant, J_0 is the limiting flux ($\text{m} \cdot \text{s}^{-1}$), and n is a constant with different
175 values for the four simple mechanisms of fouling proposed by Hermia: complete
176 blocking ($n=2$, K in min^{-1}), standard blocking ($n=1.5$, K in m^{-1}) intermediate pore
177 blocking ($n=1$, K in m^{-1}) and cake filtration ($n=0$, K in $\text{min} \cdot \text{m}^{-2}$) [36]. The choice of the
178 best model was based on the sum of squared residuals (SSR), where each residual was
179 equal to the difference between the experimental data and the value predicted by the
180 model.

181 2.4. Analytical methods

182 Humic acids were extracted from leachate according the method proposed by Thurman
183 and Malcolm [37]. Stated briefly, 10 mL of the corresponding sample were acidified
184 with HCl 1 mol/L to pH 1.0, in order to precipitate the humic acids. Then, the sample
185 was filtrated, and the solid fraction was redissolved in a 7 g/L NaOH solution until the
186 initial volume is reached. Absorbance values at 465 nm and 665 nm were measured
187 using a Helios Alpha UV-Vis spectrophotometer (Thermo Fisher Scientific, USA). A
188 calibration curve was constructed by dissolving different amounts of commercial humic
189 acid (Sigma Aldrich) in a 7 g/L NaOH solution. COD was obtained by the dichromate
190 method using a HACH DR/2500 spectrophotometer (Hach Company, USA) [38]. TOC
191 was determined using a TOC analyzer (Shimadzu TOC-V_{CSH}). The CN, which is
192 defined in equation 3 [39], was used to monitor changes in the colour of the leachate
193 during the ultrafiltration process. Spectral absorbance coefficients (SAC) are defined as
194 the ratio of the values of the respective absorbance over the cell thickness. Both CN and
195 SAC have units of cm^{-1} . This parameter was measured at 436, 525 and 620 nm using a
196 UV/Vis spectrophotometer (Thermo Scientific, Helios γ).

$$197 \quad CN = \frac{SAC_{436}^2 + SAC_{525}^2 + SAC_{620}^2}{SAC_{436} + SAC_{525} + SAC_{620}} \quad (3)$$

198 Rejection coefficients were defined as follow (eq. 4):

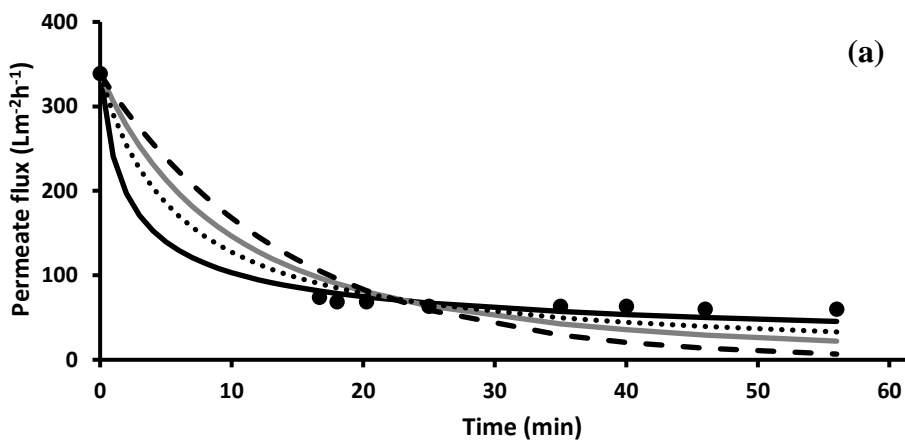
199
$$R_i = 1 - \frac{C_{P,i}}{C_{R,i}} \quad (4)$$

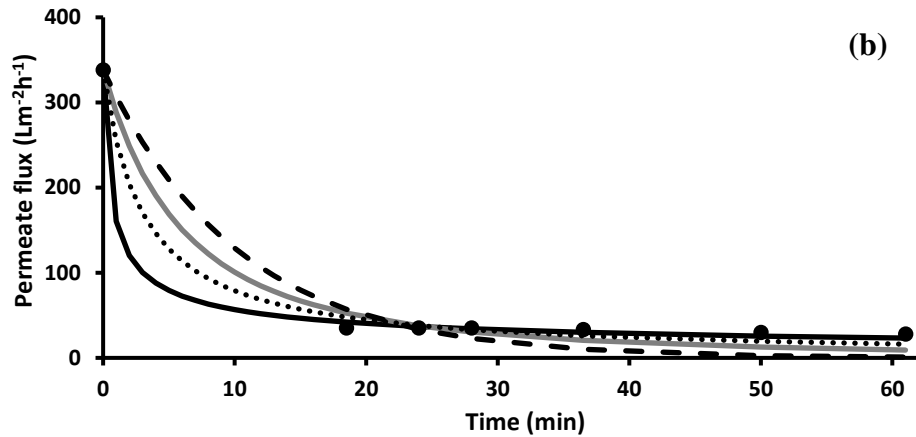
200 Where $C_{P,i}$ and $C_{R,i}$ the concentration of the analyte i in permeate and retentate,
201 respectively.

202 3. Results and discussion

203 3.1. Total Recycle mode

204 Figure 2 shows the evolution of the permeate flux with time during the ultrafiltration of
205 the mature leachate (2a) or the young one (2b) in a TR mode. The initial water
206 permeability of the membrane was 211.5 L/m² h bar. Once the filtration of the leachate
207 started, this permeability decreased rapidly for both assayed leachates, finally reaching
208 constant values of around 37.5 and 17.6 L/m² h bar for the mature and the young
209 leachate, respectively, after less than 15 min of filtration. These results correspond to
210 reductions in permeability at the end of the experiment of 82.3 and 91.7%. According to
211 several authors, these drastic flux declines, observed during the first minutes of
212 filtration, may be due to the fast accumulation on the membrane surface of a first layer
213 of fouling, which is thin but very resistant to mass transfer due to its low porosity. After
214 that, the structure of the newly formed layers is less compact, indicating the existence of
215 a porosity gradient through the cake thickness [34,40].



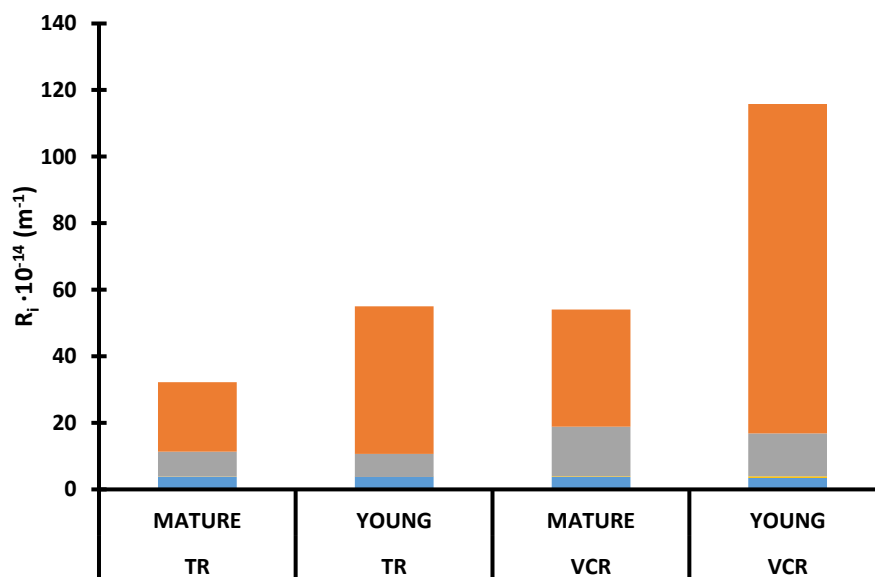


217

218 **Figure 2.** Evolution of the permeate flux (●) during the ultrafiltration of the mature (a)
 219 or young (b) leachate under TR mode. Cake model (solid black line), standard model
 220 (solid grey line), complete model (dashed black line) and intermediate model (dotted line)
 221 predictions for each of them. In all cases: 1.6 bar, 70 °C, flow rate of 5.4 L/min and cross
 222 flow velocity of 3.2 m/s.

223 Therefore, the maturation of the leachate has a positive effect on its ultrafiltration, with
 224 a twofold higher final permeability than that obtained with a young leachate. As it was
 225 previously explained, the ageing of the leachate involves a reduction in either its COD
 226 or BOD₅/COD ratio. This fact, together with the higher concentration of proteins and
 227 carbohydrates in the young leachate explain why the old leachate are more easily ultra-
 228 filtered than the young one [41,42].

229 Figure 3 shows the fouling resistances obtained for either the mature or young leachate
 230 under TR mode ultrafiltration.

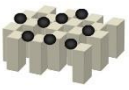


231

232 **Figure 3.** Fouling resistances obtained during the ultrafiltration of the mature (a) or young
233 (b) leachate under TR or VCR mode: R_M (■), $R_{rev.}$ (■), $R_{irrev.}$ (■) and $R_{irrecov.}$ (■). In all
234 cases: 1.6 bar, 70 °C, flow rate of 5.4 L/min and cross flow velocity of 3.2 m/s.

235 As expected from the permeability data previously commented, total resistance (R_T) for
236 the young leachate ($4.4 \cdot 10^{15} m^{-1}$) is higher than that obtained for the mature one
237 ($2.1 \cdot 10^{15} m^{-1}$). Nevertheless, these results also revealed that the flux decline due to
238 irreversible fouling is significantly lower than that caused by the reversible one. Thus,
239 calculating the $R_{rev.}/R_{irrev.}$ ratio for both leachates, the values obtained are 2.8 and 6.3
240 for the mature and young one, respectively. In this regard, it is also interesting to point
241 out that the resistances due to irreversible fouling for both experiments are somewhat
242 similar, indicating that the internal fouling is scarce and not conditioned by the stage of
243 maturation of the leachate. Considering that reversible fouling is widely associated with
244 the cake layer resistance (also known as external fouling), whereas the irreversible one
245 has to do with pore fouling resistance (or internal fouling), results show that the main
246 reason for the permeability decrease during the ultrafiltration of leachates is the external
247 fouling, this being higher for younger leachates. This fact also implies that the initial
248 membrane permeability can be easily recoverable in a high proportion after leachate
249 ultrafiltration by means of membrane relaxation, backflushing or other physical
250 cleaning techniques (standard rising) [43]. In addition, leachate age had a negligible
251 effect on both the irreversible or irrecoverable fouling. Finally, low values of $R_{irrecov.}$
252 indicated that more than 99.5% of the initial permeability is recovered after cleaning,
253 thus suggesting a long lifespan of the membrane in plant operation, either for mature or
254 young leachates, although a higher number of physical cleaning cycles would be
255 required during the ultrafiltration of the latter. If the filtration sequence (filtration
256 followed by physical cleaning) does not result in complete recovery of membrane
257 fouling status, a chemical cleaning phase is needed, which should be optimized in order
258 to maximize as much as possible the cost-efficiency of the operation.

259 Figure 2 shows the results of permeate flux and their fittings to the four simple
260 mechanisms of fouling proposed by Hermia. Additionally, Table 2 provides the values
261 of the main fitting parameters for each model as well as goodness of fit of the data to the
262 curve.

Blocking			Complete (C)	Standard (S)	Intermediate (I)	Cake (G)
Figure						
Description			Particles seal off pore entrances	Particles accumulate inside membrane on the walls of straight cylindrical pores	A portion of the particles seal off pores and the rest accumulate on the top of other deposited particles	Particles accumulate on the membrane surface
Mode	Leachate*	n	2	1.5	1	0
TR	ML	K_i	$(7.0 \pm 0.6)10^{-2}$	$(2.8 \pm 0.3)10^{-3}$	$(4.9 \pm 0.8)10^{-4}$	$(8 \pm 2)10^{-6}$
		r^2	0.93	0.97	0.98	0.995
		SRR	660	4726	9947	2333
	YL	K_i	$(9.6 \pm 0.9)10^{-2}$	$(4.5 \pm 0.6)10^{-3}$	$(9.7 \pm 0.1)10^{-4}$	$(3 \pm 1)10^{-5}$
		r^2	0.97	0.990	0.995	0.9991
		SRR	2188	850	329	59
VCR	ML	K_i	$(5.2 \pm 0.8)10^{-2}$	$(2.1 \pm 0.4)10^{-3}$	$(3.8 \pm 0.9)10^{-4}$	$(9 \pm 3)10^{-6}$
		r^2	0.92	0.95	0.97	0.990
		SRR	9461	6231	3484	1230
	YL	K_i	$(1.2 \pm 0.2)10^{-1}$	$(4.7 \pm 0.8)10^{-3}$	$(8 \pm 2)10^{-4}$	$(2.2 \pm 0.7)10^{-5}$
		r^2	0.94	0.95	0.97	0.995
		SRR	7004	5113	2587	372
<i>Units for K_i:</i>			<i>1/min</i>	<i>1/m</i>	<i>1/m</i>	<i>min/m²</i>

263 *ML: mature leachate; YL: young leachate

264 **Table 2.** Main fouling mechanisms: brief description, fitted parameters and SRR obtained
265 using the experimental data for ultrafiltration of mature and young leachates under TR or
266 VCR modes.

267 Based on the results obtained, the prevailing fouling model during the ultrafiltration of
268 leachate under TR mode corresponds to cake formation, indicating that the
269 accumulation of leachate particles occurred on the surface of the membrane in a
270 permeable cake of increasing thickness until a limit value is reached. According to this
271 mechanism, the evolution of the permeate fluxes showed in Figure 2 could be explained
272 as follows: the first phase of flux decline observed during the first few seconds or
273 minutes of operation is primarily due to concentration polarization. The second phase of
274 flux decline is slower and is attributed to the formation of a complete surface layer over
275 the initial mono-layer. The third phase represents a quasi-steady-state period, wherein
276 the flux decline occurs slowly, and may be due to the consolidation of the fouling layer
277 due to a balance between the deposition of foulants on the cake and their removal due to
278 the shear stress caused by the cross flow [20]. The final achievement of a final cake
279 with an almost constant thickness is consistent with the prevalence of an external
280 fouling observed from the analysis of the resistance-in-series mode. Ma et al. [44] also

281 found that cake filtration was the main fouling mechanism involved during the
282 ultrafiltration of humic acid with and without addition of inorganic salts. Syzdek and
283 Ahlert [14] reported some results during the ultrafiltration of a high-strength industrial
284 landfill leachate which suggested the predominance of cake formation as main fouling
285 mechanism as well. For example, the fouling layer did not block the passage of organic
286 carbon across the membrane, but only created a pressure drop that resulted in a lower
287 flux. The occurrence of this fouling mechanism poses operational implications. When
288 working with a non-foulant stream, a linear relationship between applied TMP and flux
289 is assumed. Nonetheless, if fouling particles present in the stream are larger than the
290 membrane pore size, a fouling cake will eventually deposit on the membrane surface.
291 This phenomenon occurs more drastically when higher pressures are applied,
292 compressing the fouling cake and minimizing membrane flux [45]. It has been reported
293 that, in these cases, Reynolds number happens to be more relevant for flux improving
294 that applied pressure [46], making it possible to minimize the fouling layer by
295 increasing the shear at the membrane surface.

296 Several authors reported that fouling of the majority of membrane processes applied to
297 leachate treatment was mainly due to the presence of humic substances in the leachate
298 organic fraction [22,47]. If the formation of an external fouling layer, as suggested by
299 previous fouling models, is assumed, then it is also reasonable to suppose that humic
300 acids are mainly retained on the membrane surface. It should be highlighted that
301 interactions between humic acids (as well as other natural organic matter) and the
302 membrane are of hydrophobic nature [48], and thus a high ionic strength of the stream
303 fosters membrane fouling caused by humic acid [31].

304 As the concentrations of humic acids are quite similar in both leachates because the
305 biodegradability of these compounds is almost null, the lower permeability of the young
306 leachate should be associated with the species which are biologically degraded during
307 its maturation. Considering that the fouling associated with humic substances is
308 approximately the same, the leachates which are degraded during the landfill maturation
309 are responsible for the 75% (calculation based on K_i) of the fouling observed during the
310 ultrafiltration of the leachate in TR mode.

311 3.2. Volume Concentration Ratio mode

312 In order to gather information about the influence of solute concentration on the
313 permeability and membrane rejection during the ultrafiltration of either the young or
314 mature leachates, a set of experiments without permeate recirculation to the feed tank
315 were also carried out. It is worth noting here that, whereas the TR mode simulates a
316 continuous filtration, the aim of these experiments, named as VCR mode, is to study the
317 batch filtration and decide the most convenient solute concentration in a continuous
318 filtration.

319 Figure 4 shows the evolution with time of the permeate flux during the VCR mode
320 ultrafiltration of a mature (a) or a young leachate (b). As in the case of TR, the decline
321 in the permeate flux for the young leachate was stronger than that obtained for the
322 mature one. Again, the reduction in the permeability mainly occurred during the first
323 minutes of filtration. Nevertheless, the permeability losses were more noticeable for the
324 VCR mode filtration than for the TR mode operations, as expected due to the gradual
325 increase in the concentration of the feed. So, the final permeate fluxes for VCR mode
326 experiments with mature or young leachates were a 41 and 55% lower than those
327 obtained during the ultrafiltration in TR mode.

328 These results indicate that the fouling resistance, $(R_T - R_M)$, during the batch
329 ultrafiltration (VCR mode) is approximately twofold higher than that of the continuous
330 one (TR mode) under the same time of filtration (60 min). More specifically, the fouling
331 resistances obtained during TR and VCR mode experiments were $2.8 \cdot 10^{15}$ and $5.0 \cdot 10^{15}$
332 m^{-1} for the mature leachate and $5.1 \cdot 10^{15}$ and $11.2 \cdot 10^{15} \text{ m}^{-1}$ for the young one,
333 respectively. Using the resistance-in-series model (see Figure 3), it can be deduced that
334 the main contribution to this resistance is due to reversible fouling, which represented
335 70% and 88% of the total fouling for the mature and young leachates, respectively.
336 These percentages were pretty similar to those obtained under TR mode. Nevertheless,
337 the irreversible fouling during the batch ultrafiltration increased substantially in
338 comparison to the continuous one, although no significant differences were found
339 between young and mature leachates (Figure 3). Regarding the irrecoverable fouling, its
340 contribution to the total fouling was negligible for both leachates.

341

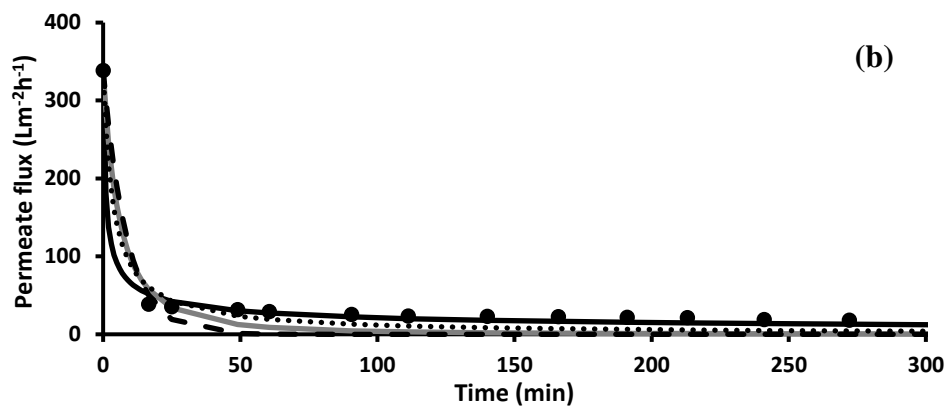
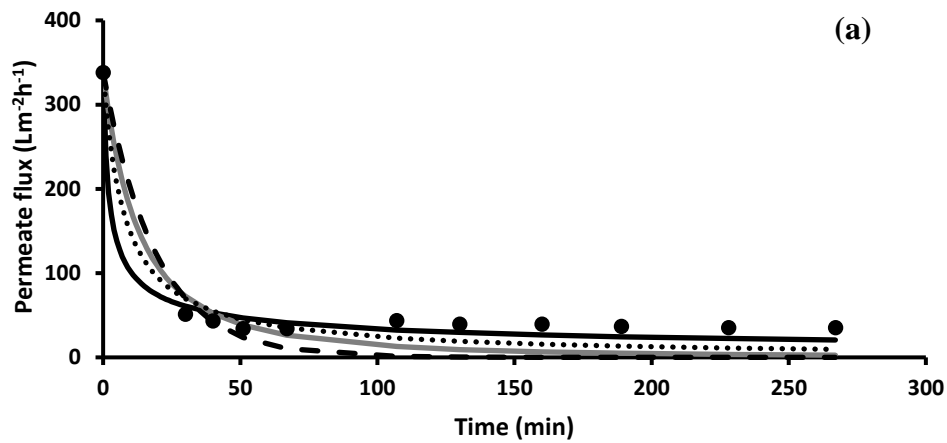
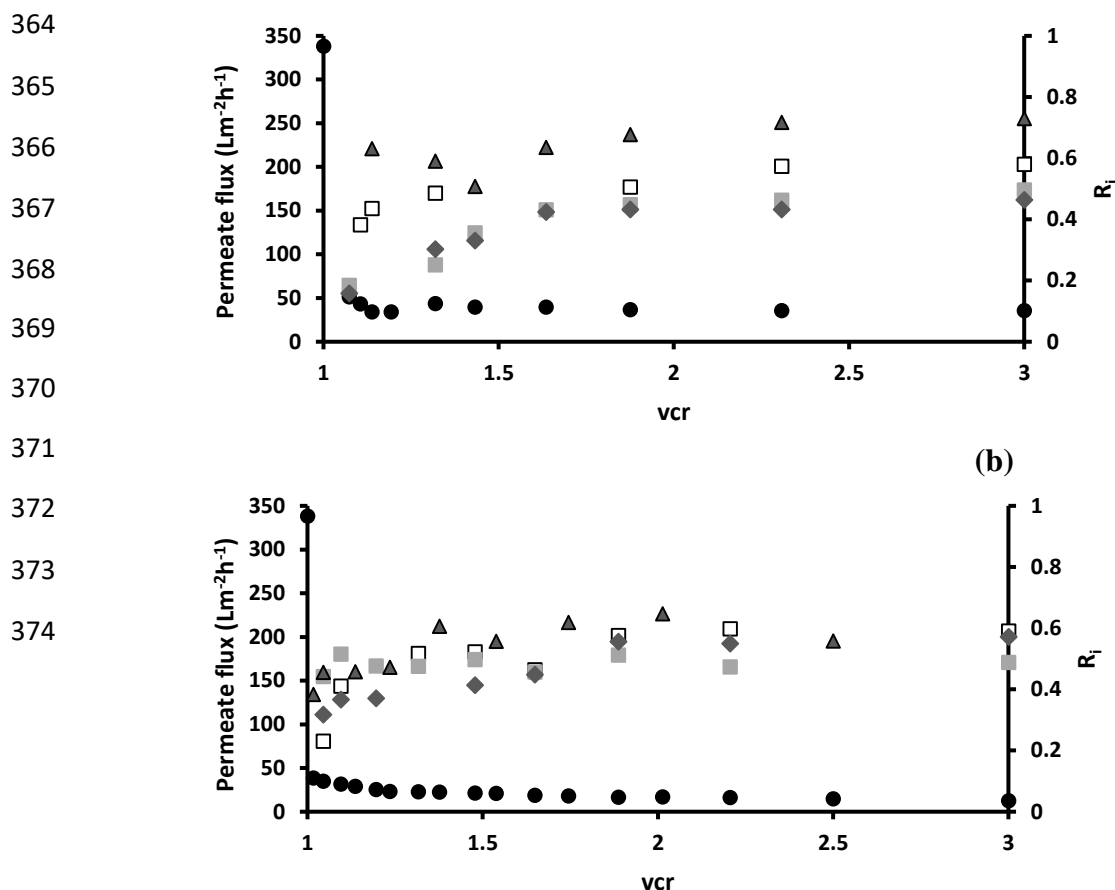


Figure 4. Evolution of the permeate flux (●) during the ultrafiltration of the mature (a) or young (b) leachate under VCR mode. Cake model (solid black line), standard model (solid grey line), complete model (dashed black line) and intermediate model (dotted line) predictions for each of them. In all cases: 1.6 bar, 70 °C, flow rate of 5.4 L/min and cross flow velocity of 3.2 m/s.

Using again the individual fouling models proposed by Hermia [35] (Figure 4 and Table 2), the loss of permeability during the batch ultrafiltration of either the mature or young leachate was mainly attributed to the cake formation mechanism, as with the continuous one. The predominance of this fouling model is consistent with the high proportion of reversible fouling [49].

Figure 5 shows the evolution of the rejection coefficients for COD (R_{COD}), TOC (R_{TOC}), colour (R_{CN}) and humic acids (R_{HA}) as well as the permeate flux with the VCR mode during the ultrafiltration of either a mature or young leachate.

(a)



375 **Figure 5.** Evolution of the rejection coefficients for COD (■), TOC (◆), colour (▲) and
 376 humic acids (□) and permeate flux (●) with the VCR mode during the ultrafiltration of
 377 either a mature (a) or a young leachate (b). In all cases: 1.6 bar, 70 °C, flow rate of 5.4
 378 L/min and cross flow velocity of 3.2 m/s.

379 Dealing first with permeate fluxes, the evolutions of these with VCR are the expected
 380 ones for both leachates, differentiating three periods. Thus, a rapid flux drop was
 381 observed initially, which was mainly attributed to concentration polarization, followed
 382 by a less marked decrease in the flux due to irreversible fouling and a final period
 383 corresponding to a small flux decrease. As can be seen in Figure 5, the short duration of
 384 the second period suggests that internal fouling is not significant, as it was deduced
 385 from the analysis of resistances. Regarding the latter period, it is usually associated with
 386 the foulant deposition on the membrane surface, that is to say, the reversible fouling
 387 [50]. During this stage, approximately constant fouling rates of $4.3 \cdot 10^{-3}$ or $7.9 \cdot 10^{-3} \text{ m}^{-1}\text{h}^{-1}$
 388 ¹ were observed for the mature or the young leachate, respectively.

389 Regarding the rejection coefficients, their evolutions differed between leachates. For
 390 instance, the COD rejection for the mature leachate showed an approximately sigmoidal

391 shape, from an initial value of 18.5% to a final one of 49.6%, with the faster increase at
392 VCR ranging from 1.2 to 1.7. Nevertheless, this parameter seemed to remain
393 approximately constant during the ultrafiltration of the young leachate, although a slight
394 increase was perceived at the beginning of the filtration. Concerning R_{TOC} , it showed
395 similar values to R_{COD} throughout the filtration experiment. Nevertheless, in the case of
396 the young one, the R_{COD} values were slightly higher than that of the R_{TOC} at the
397 beginning of the ultrafiltration. In regard to CN, the rejections were significantly higher
398 for the mature leachate, although a decrease in the R_{CN} for mature leachate during the
399 early stages of the operation could be seen. These differences in the evolution of the
400 COD, TOC and CN rejections for both leachates can be explained on the basis of their
401 composition. A more in-depth and detailed discussion of this statement will be carried
402 out in the next section.

403 3.3. Fouling mechanism

404 The previous observations on permeate fluxes and rejection coefficients seem to suggest
405 that there is clear connection between ultrafiltration performance and the changes in the
406 leachate composition due to landfill ageing.

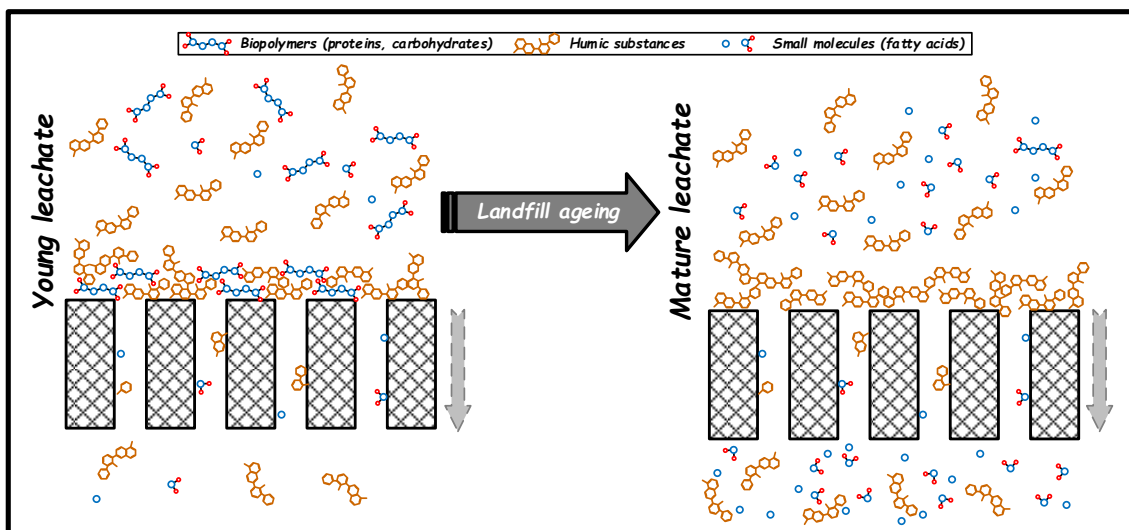
407 In this regard and before developing this relationship, it is interesting to mention that
408 landfills undergo at least four stages of decomposition during their ageing: an initial
409 aerobic phase, an anaerobic acid phase, an initial methanogenic phase and, finally, a
410 stable methanogenic phase, thus existing a strong relationship between the state of
411 refuse decomposition and its corresponding leachate characteristics [51]. On the basis of
412 size exclusion chromatography results, Aftab and Hur [52] proposed that leachates are
413 composed by five different fractions: biopolymers (>10 kDa), humic substances
414 (approx. 1 kDa), building blocks (300–500 Da), and low molecular neutrals and acids
415 (<350 Da). As the landfill is becoming older, biopolymers are broken up into building
416 blocks and these are decomposed and transformed into simple molecules, such as fatty
417 acids, carbon dioxide and methane, whereas humic substances are hardly modified due
418 to their recalcitrant character [17,53] (see Figure 6). Therefore, a high relative
419 abundance of low molecular weight compounds in the mature leachate but not in the
420 young one is accepted. In this sense, Mohammadzadeh and Clark (2008) reported that
421 leachates generated in an area of old wastes were mainly composed of humic substances
422 and simple fatty acids (mostly acetic and propionic) [53]. Taking into account that COD

423 and TOC measurements include all the organic compounds, the small fatty acids easily
424 passed through the membrane during the first minutes of ultrafiltration of the mature
425 leachate, thus increasing the permeate COD and TOC and reducing the initial R_{COD} and
426 R_{TOC} , as it is observed in Figure 5. Meanwhile, the proportion of compounds with
427 higher molecular weight in the retentate increased. Once most of the fatty acids had
428 already been removed, the COD and TOC values in the permeate mainly depended on
429 the presence of humic substances on it. Obviously, this causes a progressive increase in
430 the COD and TOC rejection, thereby the rejection coefficients of the compounds tend to
431 approximate to that of the higher molecular size, that is to say, to the humic acids one
432 (R_{HA}), thus explaining the sigmoidal evolution of R_{COD} and R_{TOC} observed in Figure 5.
433 At this point, it should be pointed out that the increase in the humic acids rejection
434 during the first minutes of filtration was probably due to the rapid development of a
435 fouling layer on the membrane surface, as explained above. This external fouling layer
436 is mainly made up of humic acids and acts as a dynamic membrane, reducing the
437 permeability and increasing R_{HA} [44,54]. The additional barrier would not have
438 influence on the pass of small molecules, such as the fatty acids, so its reject coefficient
439 would not be affected. Once the cake was formed, its compaction and/or the
440 consolidation of irreversible fouling are likely the main reasons why the R_{HA} slightly
441 increased after the external fouling layer was formed (Figure 5) [50,55]. With regard to
442 the high values of R_{CN} , it should be taken into account that mature leachate is mainly
443 composed of humic acids, which are highly coloured, and simple fatty acids, which are
444 colourless. Therefore, permeate results in an almost colourless stream, thus achieving a
445 high colour retention due to humic acid retention.

446 On the other hand, the composition of a young leachate is more complex. When
447 compared with mature leachates, the lower relative content in small molecules of the
448 young ones can also explain the results depicted in Figure 5. Thus, the small variation in
449 R_{COD} with VCR observed for the young leachate, instead of the sigmoidal tendency of
450 the mature one, can be attributed to the higher abundance of high molecular weight
451 compounds and their cohesive interactions facilitated by the higher ionic strength of the
452 young leachate [56]. Taking into account that the molecular weight cut-off of the
453 membrane is 150 kDa and the predominance of biopolymers (>10 kDa) and humic acids
454 (approx. 1 kDa) in the young leachate, COD and humic acids rejections should be pretty
455 similar to each other, as was experimentally proved (Figure 5) [4,52].

456 As for R_{CN} , lower values were observed in comparison to that of the mature leachate.
457 This can be explained considering the chemical nature of the young leachate. This
458 stream is highly complex, as opposed to the mature leachate which, as it was previously
459 mentioned, is mainly made up of humic acids and simple fatty acids. Thus, both
460 retentate and permeate will be richer in coloured species, therefore, reducing colour
461 differences between these streams.

462 Finally, the experimental evidence that total resistance for the young leachate is higher
463 than that of the mature one can be also linked to the leachate composition. Young
464 leachate has a high proportion of biopolymers (>10 kDa), while organic matter in
465 mature leachate consists basically of humic substances. Renou et al. (2009) reported that
466 the major cause of ceramic membrane fouling during the ultrafiltration of landfill
467 leachate was the formation of precipitated humic acid on the surface of the membrane,
468 fostered by the presence of calcium ions [22]. Nevertheless, during the filtration of
469 young leachate, interactions between the deposited humic acid and biopolymers present
470 in the stream are expected, generating a thicker, less permeable fouling cake (Figure 2).
471 In this sense, Jermann et al. (2007) observed that humic acids could act as a bridge
472 between alginate and membrane, resulting in a more stable and less reversible fouling
473 layer [41]. In a similar way, Xiao et al. (2013) also reported the interaction proneness
474 between humic acids, polysaccharides and proteins [42].



476 **Figure 6.** Proposed effect of the landfill age on the ultrafiltration of the leachate
477 generated.

478 Conclusions

479 Results suggest that there is a clear connection between ultrafiltration performance and
480 the changes in the leachate composition due to landfill ageing. Both young and mature
481 leachates cause a very steep permeate flux decline, during the first minutes of filtration,
482 probably due to the fast accumulation on the membrane surface of a first layer of
483 fouling. In a second stage, the flux declines slower, caused by the consolidation of the
484 fouling layer due to a balance between the deposition of foulants on the cake and their
485 removal produced by the shear stress of the cross flow.

486 The maturation of the leachate has a positive effect on the permeability, with a twofold
487 higher final permeability than that obtained with a young leachate. This finding is likely
488 related to the higher concentration of proteins and carbohydrates in the young leachate.
489 The main reason for the decrease of permeability during the ultrafiltration of leachates
490 is the external fouling, this being higher for younger leachates. Resistance-in-series
491 analysis demonstrated that the loss of permeability was mainly due to reversible fouling.
492 Either irrecoverable or internal fouling were scarce and not determined by the stage of
493 maturation of the leachate. This leads to suggest a long lifespan of the membrane in
494 plant operation, since more than 99.5% of the initial permeability can be recovered after
495 cleaning.

496 The prevailing fouling model during the ultrafiltration of both leachates is the
497 corresponding to cake formation, either under TR or VCR modes. COD rejection for the
498 mature leachate showed an approximately sigmoidal shape, from an initial value of
499 18.5% to a final one of 49.6%, with the faster increase for VCR ranging from 1.2 to 1.7.
500 The main reason for this behaviour is due to the fatty acids are not retained by the UF
501 membrane. On the other hand, COD rejection remains approximately constant during
502 the ultrafiltration of the young leachate (48%), which can be attributed to the presence
503 of higher molecular weight compounds in its composition.

504

505 **Acknowledgements**

506 The authors are grateful for the financial support from the Spanish Ministry of Economy
507 and Competitiveness (MINECO) through Project CTM2015-63864-R and FEDER
508 funds from European Union. Authors also acknowledge the financial support from the
509 Employment, Industry and Tourism Office of Principality of Asturias (Spain) through
510 the project GRUPIN IDI/2018/000127. The author Daniel Núñez thanks the Principality

511 of Asturias for their financial support through the Severo Ochoa scholarship n° BP19-
512 093.

513

514 **References**

515 [1] D.S. Fernández, M.E. Puchulu, S.M. Georgieff, Identification and assessment of
516 water pollution as a consequence of a leachate plume migration from a municipal
517 landfill site (Tucumán, Argentina), *Environ. Geochem. Health.* 36 (2014) 489–
518 503. doi:10.1007/s10653-013-9576-1.

519 [2] C.M. Moody, T.G. Townsend, A comparison of landfill leachates based on waste
520 composition, *Waste Manag.* 63 (2017) 267–274.
521 doi:10.1016/j.wasman.2016.09.020.

522 [3] L.M. Chu, K.C. Cheung, M.H. Wong, Variations in the chemical properties of
523 landfill leachate, *Environ. Manage.* 18 (1994) 105–117.
524 doi:10.1007/BF02393753.

525 [4] D. Kulikowska, E. Klimiuk, The effect of landfill age on municipal leachate
526 composition, *Bioresour. Technol.* 99 (2008) 5981–5985.
527 doi:10.1016/j.biortech.2007.10.015.

528 [5] C.B. Öman, C. Junestedt, Chemical characterization of landfill leachates - 400
529 parameters and compounds, *Waste Manag.* 28 (2008) 1876–1891.
530 doi:10.1016/j.wasman.2007.06.018.

531 [6] J. Wiszniowski, D. Robert, J. Surmacz-Gorska, K. Miksch, J. V. Weber, Landfill
532 leachate treatment methods: A review, *Environ. Chem. Lett.* 4 (2006) 51–61.
533 doi:10.1007/s10311-005-0016-z.

534 [7] Y. Peng, Perspectives on technology for landfill leachate treatment, *Arab. J.*
535 *Chem.* 10 (2017) S2567–S2574. doi:10.1016/j.arabjc.2013.09.031.

536 [8] V. Oloibiri, M. Chys, S. De Wandel, K. Demeestere, S.W.H. Van Hulle,
537 Removal of organic matter and ammonium from landfill leachate through
538 different scenarios: Operational cost evaluation in a full-scale case study of a
539 Flemish landfill, *J. Environ. Manage.* 203 (2017) 774–781.
540 doi:10.1016/j.jenvman.2016.09.055.

- 541 [9] R.B. Brennan, E. Clifford, C. Devroedt, L. Morrison, M.G. Healy, Treatment of
542 landfill leachate in municipal wastewater treatment plants and impacts on effluent
543 ammonium concentrations, *J. Environ. Manage.* 188 (2017) 64–72.
544 doi:10.1016/j.jenvman.2016.11.055.
- 545 [10] S. Renou, J.G. Givaudan, S. Poulain, F. Dirassouyan, P. Moulin, Landfill
546 leachate treatment: Review and opportunity, *J. Hazard. Mater.* 150 (2008) 468–
547 493. doi:10.1016/j.jhazmat.2007.09.077.
- 548 [11] X. Shi, G. Tal, N.P. Hankins, V. Gitis, Fouling and cleaning of ultrafiltration
549 membranes: A review, *J. Water Process Eng.* 1 (2014) 121–138.
550 doi:10.1016/j.jwpe.2014.04.003.
- 551 [12] D. Kulikowska, M. Zielińska, K. Konopka, Treatment of stabilized landfill
552 leachate in an integrated adsorption–fine-ultrafiltration system, *Int. J. Environ.*
553 *Sci. Technol.* 16 (2019) 423–430. doi:10.1007/s13762-018-1685-z.
- 554 [13] K. Tabet, P. Moulin, J.D. Vilomet, A. Amberto, F. Charbit, Purification of
555 landfill leachate with membrane processes: Preliminary studies for an industrial
556 plant, *Sep. Sci. Technol.* 37 (2002) 1041–1063. doi:10.1081/SS-120002240.
- 557 [14] A.C. Syzdek, R.C. Ahlert, Separation of landfill leachate with polymeric
558 ultrafiltration membranes, *J. Hazard. Mater.* 9 (1984) 209–220.
559 doi:10.1016/0304-3894(84)80018-7.
- 560 [15] D. Dolar, K. Košutić, T. Strmecky, Hybrid processes for treatment of landfill
561 leachate: Coagulation/UF/NF-RO and adsorption/UF/NF-RO, *Sep. Purif.*
562 *Technol.* 168 (2016) 39–46. doi:10.1016/j.seppur.2016.05.016.
- 563 [16] D. Cingolani, A.L. Eusebi, P. Battistoni, Osmosis process for leachate treatment
564 in industrial platform: Economic and performances evaluations to zero liquid
565 discharge, *J. Environ. Manage.* 203 (2017) 782–790.
566 doi:10.1016/j.jenvman.2016.05.012.
- 567 [17] RO & UF membranes: Market opportunities in landfill leachate, *Water*
568 *Wastewater Int.* 27 (2012) 46–49.
- 569 [18] Y.D. Xu, D.B. Yue, Y. Zhu, Y.F. Nie, Fractionation of dissolved organic matter
570 in mature landfill leachate and its recycling by ultrafiltration and evaporation

- 571 combined processes, *Chemosphere*. 64 (2006) 903–911.
572 doi:10.1016/j.chemosphere.2006.01.039.
- 573 [19] M.C. Cammarota, L. Yokoyama, J.C. Campos, Ultrafiltration, chemical and
574 biological oxidation as process combination for the treatment of municipal
575 landfill leachate, *Desalin. Water Treat.* 3 (2009) 50–57.
576 doi:10.5004/dwt.2009.440.
- 577 [20] M. Pirbazari, V. Ravindran, B.N. Badriyha, S.H. Kim, Hybrid membrane
578 filtration process for leachate treatment, *Water Res.* 30 (1996) 2691–2706.
579 doi:10.1016/S0043-1354(96)00183-2.
- 580 [21] C.F. Lin, Y.J. Huang, O.J. Hao, Ultrafiltration processes for removing humic
581 substances: Effect of molecular weight fractions and PAC treatment, *Water Res.*
582 33 (1999) 1252–1264. doi:10.1016/S0043-1354(98)00322-4.
- 583 [22] S. Renou, S. Poulain, J.G. Givaudan, P. Moulin, Amelioration of ultrafiltration
584 process by lime treatment: Case of landfill leachate, *Desalination*. 249 (2009) 72–
585 82. doi:10.1016/j.desal.2008.09.007.
- 586 [23] Y. Xu, C. Chen, X. Li, J. Lin, Y. Liao, Z. Jin, Recovery of humic substances
587 from leachate nanofiltration concentrate by a two-stage process of tight
588 ultrafiltration membrane, *J. Clean. Prod.* 161 (2017) 84–94.
589 doi:10.1016/j.jclepro.2017.05.095.
- 590 [24] K.W. Pi, Z. Li, D.J. Wan, L.X. Gao, Pretreatment of municipal landfill leachate
591 by a combined process, *Process Saf. Environ. Prot.* 87 (2009) 191–196.
592 doi:10.1016/j.psep.2009.01.002.
- 593 [25] O. Primo, A. Rueda, M.J. Rivero, I. Ortiz, An integrated process, fenton reaction
594 - Ultrafiltration, for the treatment of landfill leachate: Pilot plant operation and
595 analysis, *Ind. Eng. Chem. Res.* 47 (2008) 946–952. doi:10.1021/ie071111a.
- 596 [26] P. Oulego, S. Collado, A. Laca, M. Díaz, Impact of leachate composition on the
597 advanced oxidation treatment, *Water Res.* 88 (2016) 389–402.
598 doi:10.1016/j.watres.2015.09.048.
- 599 [27] B.P. Naveen, P. V. Sivapullaiyah, T.G. Sitharami, Effect of aging on the leachate
600 characteristics from municipal solid waste landfill, in: 15th Asian Reg. Conf. Soil

- 601 Mech. Geotech. Eng. ARC 2015 New Innov. Sustain., 2015: pp. 1940–1945.
602 doi:10.3208/jgssp.IND-06.
- 603 [28] S.H. Park, Y.G. Park, J.L. Lim, S. Kim, Evaluation of ceramic membrane
604 applications for water treatment plants with a life cycle cost analysis, *Desalin.*
605 *Water Treat.* 54 (2015) 973–979. doi:10.1080/19443994.2014.912162.
- 606 [29] S. Khan, J. Kim, A. Sotto, B. Van der Bruggen, Humic acid fouling in a
607 submerged photocatalytic membrane reactor with binary TiO₂-ZrO₂ particles, *J.*
608 *Ind. Eng. Chem.* 21 (2015) 779–786. doi:10.1016/j.jiec.2014.04.012.
- 609 [30] J. Guo, S. Khan, S.H. Cho, J. Kim, ZnS nanoparticles as new additive for
610 polyethersulfone membrane in humic acid filtration, *J. Ind. Eng. Chem.* 79
611 (2019) 71–78. doi:10.1016/j.jiec.2019.05.015.
- 612 [31] W. Yuan, A.L. Zydney, Humic acid fouling during ultrafiltration, *Environ. Sci.*
613 *Technol.* 34 (2000) 5043–5050. doi:10.1021/es0012366.
- 614 [32] I. Sutzkover-Gutman, D. Hasson, R. Semiat, Humic substances fouling in
615 ultrafiltration processes, *Desalination.* 261 (2010) 218–231.
616 doi:10.1016/j.desal.2010.05.008.
- 617 [33] S.J. Judd, C. Judd, *The MBR Book*, 2011. doi:10.1016/B978-1-85617-481-
618 7.X5000-4.
- 619 [34] I. Rosas, S. Collado, A. Gutiérrez, M. Díaz, Fouling mechanisms of
620 *Pseudomonas putida* on PES microfiltration membranes, *J. Memb. Sci.* 465
621 (2014) 27–33. doi:10.1016/j.memsci.2014.04.002.
- 622 [35] J. HERMIA, Constant Pressure Blocking Filtration Laws - Application Topower-
623 Law Non-Newtonian Fluids., *Trans Inst Chem Eng.* V 60 (1982) 183–187.
- 624 [36] M. Abbasi, R.S. Mohammad, A. Salahi, B. Mirza, Modeling of membrane
625 fouling and flux decline in microfiltration of oily wastewater using ceramic
626 membranes, *Chem. Eng. Commun.* 199 (2012) 78–93.
627 doi:10.1080/00986445.2011.570391.
- 628 [37] E.M. Thurman, R.L. Malcolm, Preparative Isolation of Aquatic Humic
629 Substances, *Environ. Sci. Technol.* 15 (1981) 463–466.
630 doi:10.1021/es00086a012.

- 631 [38] L. Vinet, A. Zhedanov, A “missing” family of classical orthogonal polynomials,
632 2011. doi:10.1088/1751-8113/44/8/085201.
- 633 [39] C. Tizaoui, L. Bouselmi, L. Mansouri, A. Ghrabi, Landfill leachate treatment
634 with ozone and ozone/hydrogen peroxide systems, *J. Hazard. Mater.* 140 (2007)
635 316–324. doi:10.1016/j.jhazmat.2006.09.023.
- 636 [40] V. V. Tarabara, I. Koyuncu, M.R. Wiesner, Effect of hydrodynamics and solution
637 ionic strength on permeate flux in cross-flow filtration: Direct experimental
638 observation of filter cake cross-sections, *J. Memb. Sci.* 241 (2004) 65–78.
639 doi:10.1016/j.memsci.2004.04.030.
- 640 [41] D. Jermann, W. Pronk, S. Meylan, M. Boller, Interplay of different NOM fouling
641 mechanisms during ultrafiltration for drinking water production, *Water Res.* 41
642 (2007) 1713–1722. doi:10.1016/j.watres.2006.12.030.
- 643 [42] F. Xiao, P. Xiao, W.J. Zhang, D.S. Wang, Identification of key factors affecting
644 the organic fouling on low-pressure ultrafiltration membranes, *J. Memb. Sci.* 447
645 (2013) 144–152. doi:10.1016/j.memsci.2013.07.040.
- 646 [43] M. Kraume, D. Wedi, J. Schaller, V. Iversen, A. Drews, Fouling in MBR: What
647 use are lab investigations for full scale operation?, *Desalination.* 236 (2009) 94–
648 103. doi:10.1016/j.desal.2007.10.055.
- 649 [44] B. Ma, Y. Ding, W. Li, C. Hu, M. Yang, H. Liu, J. Qu, Ultrafiltration membrane
650 fouling induced by humic acid with typical inorganic salts, *Chemosphere.* 197
651 (2018) 793–802. doi:10.1016/j.chemosphere.2018.01.037.
- 652 [45] M. Said, A. Ahmad, A.W. Mohammad, M.T.M. Nor, S.R. Sheikh Abdullah,
653 Blocking mechanism of PES membrane during ultrafiltration of POME, *J. Ind.*
654 *Eng. Chem.* 21 (2015) 182–188. doi:10.1016/j.jiec.2014.02.023.
- 655 [46] H. Rezaei, F.Z. Ashtiani, A. Fouladitajar, Effects of operating parameters on
656 fouling mechanism and membrane flux in cross-flow microfiltration of whey,
657 *Desalination.* 274 (2011) 262–271. doi:10.1016/j.desal.2011.02.015.
- 658 [47] C.S. Slater, R.C. Ahlert, C.G. Uchirin, Applications of reverse osmosis to
659 complex industrial wastewater treatment, *Desalination.* 48 (1983) 171–187.
660 doi:10.1016/0011-9164(83)80015-0.

- 661 [48] D.H. Kim, H.K. Shon, G. Sharma, J. Cho, Charge effect of natural organic matter
662 for ultrafiltration and nanofiltration membranes, *J. Ind. Eng. Chem.* 17 (2011)
663 109–113. doi:10.1016/j.jiec.2010.12.006.
- 664 [49] T. Janus, B. Ulanicki, A behavioural membrane fouling model for integrated
665 simulation of membrane bioreactors for wastewater treatment, in: *Procedia Eng.*,
666 2015: pp. 1328–1337. doi:10.1016/j.proeng.2015.08.964.
- 667 [50] A.R. Taherian, M. Mondor, F. Lamarche, Enhancing nutritional values and
668 functional properties of yellow pea protein via membrane processing, *Peas*
669 *Cultiv. Var. Nutr. Uses.* (2012) 1–48.
- 670 [51] P. Kjeldsen, M.A. Barlaz, A.P. Rooker, A. Baun, A. Ledin, T.H. Christensen,
671 Present and long-term composition of MSW landfill leachate: A review, *Crit.*
672 *Rev. Environ. Sci. Technol.* 32 (2002) 297–336.
673 doi:10.1080/10643380290813462.
- 674 [52] B. Aftab, J. Hur, Unraveling complex removal behavior of landfill leachate upon
675 the treatments of Fenton oxidation and MIEX[®] via two-dimensional correlation
676 size exclusion chromatography (2D-CoSEC), *J. Hazard. Mater.* 362 (2019) 36–
677 44. doi:10.1016/j.jhazmat.2018.09.017.
- 678 [53] H. Mohammadzadeh, I. Clark, Degradation pathways of dissolved carbon in
679 landfill leachate traced with compound-specific ¹³C analysis of DOC, *Isotopes*
680 *Environ. Health Stud.* 44 (2008) 267–294. doi:10.1080/10256010802309814.
- 681 [54] M.E. Ersahin, H. Ozgun, R.K. Dereli, I. Ozturk, K. Roest, J.B. van Lier, A
682 review on dynamic membrane filtration: Materials, applications and future
683 perspectives, *Bioresour. Technol.* 122 (2012) 196–206.
684 doi:10.1016/j.biortech.2012.03.086.
- 685 [55] C. de Moraes Coutinho, M.C. Chiu, R.C. Basso, A.P.B. Ribeiro, L.A.G.
686 Gonçalves, L.A. Viotto, State of art of the application of membrane technology
687 to vegetable oils: A review, *Food Res. Int.* 42 (2009) 536–550.
688 doi:10.1016/j.foodres.2009.02.010.
- 689 [56] T. Lin, Z.J. Lu, W. Chen, Interaction mechanisms of humic acid combined with
690 calcium ions on membrane fouling at different conditions in an ultrafiltration
691 system, *Desalination.* 357 (2015) 26–35. doi:10.1016/j.desal.2014.11.007.

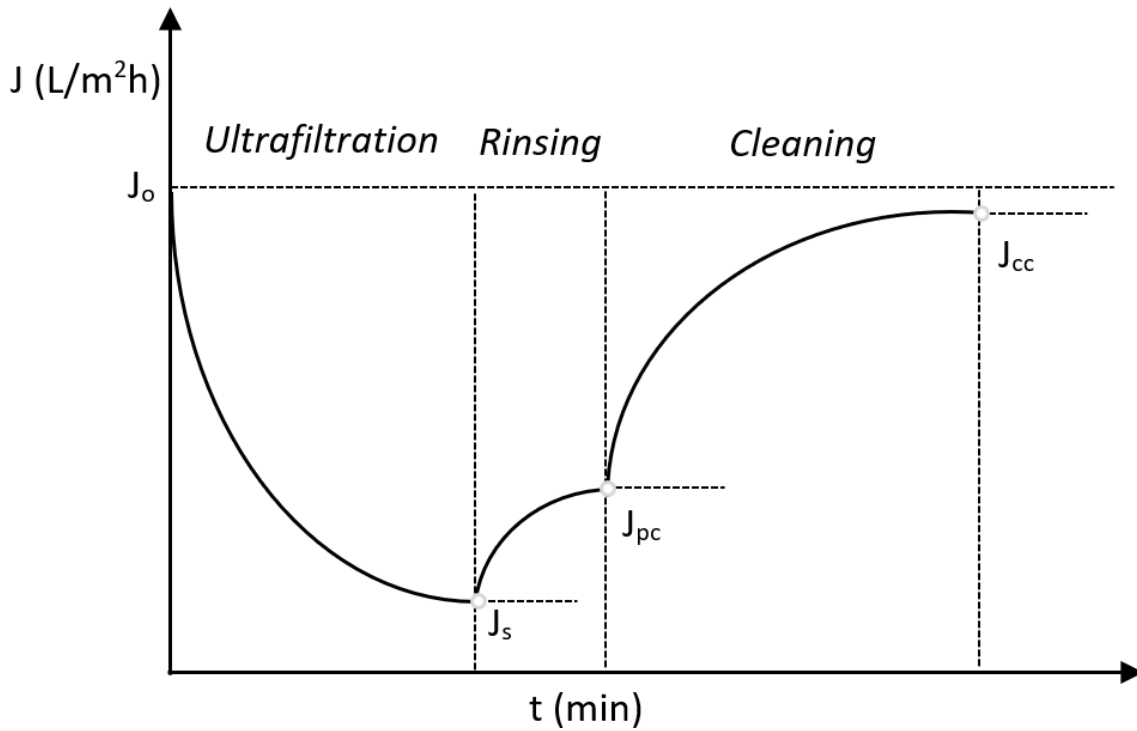
692 [57] M.A. Argüello, S. Álvarez, F.A. Riera, R. Álvarez, Enzymatic cleaning of
693 inorganic ultrafiltration membranes used for whey protein fractionation, J.
694 Memb. Sci. 216 (2003) 121–134. doi:10.1016/S0376-7388(03)00064-4.

695

696 **Appendix**

697 **Determination of R_m , R_{rev} , R_{irrev} and $R_{irrecov}$**

698 Figure A.1 illustrates the evolution of J throughout the experiments. Initial flux (J_o), flux
 699 after leachate ultrafiltration and before cleaning (J_s), flux after physical cleaning with
 700 water (J_{pc}) and flux after chemical cleaning (J_{cc}) are measured to calculate the resistances
 701 model.



702

703 **Figure A1.** Evolution of flux during ultrafiltration, rinsing and cleaning.

704 According to Darcy's law:

705
$$R = \frac{\Delta P}{\mu J}$$

706 Where R is the hydraulic resistance of the membrane, ΔP is the TMP, μ is the viscosity,
 707 and J is the permeate flux. Also, according to the resistances-in-series model, total
 708 resistance can be expressed as a sum of different resistances (eq. A.1):

709
$$R_s = R_m + R_{rev} + R_{irrev} + R_{irrecov} \quad (A.1)$$

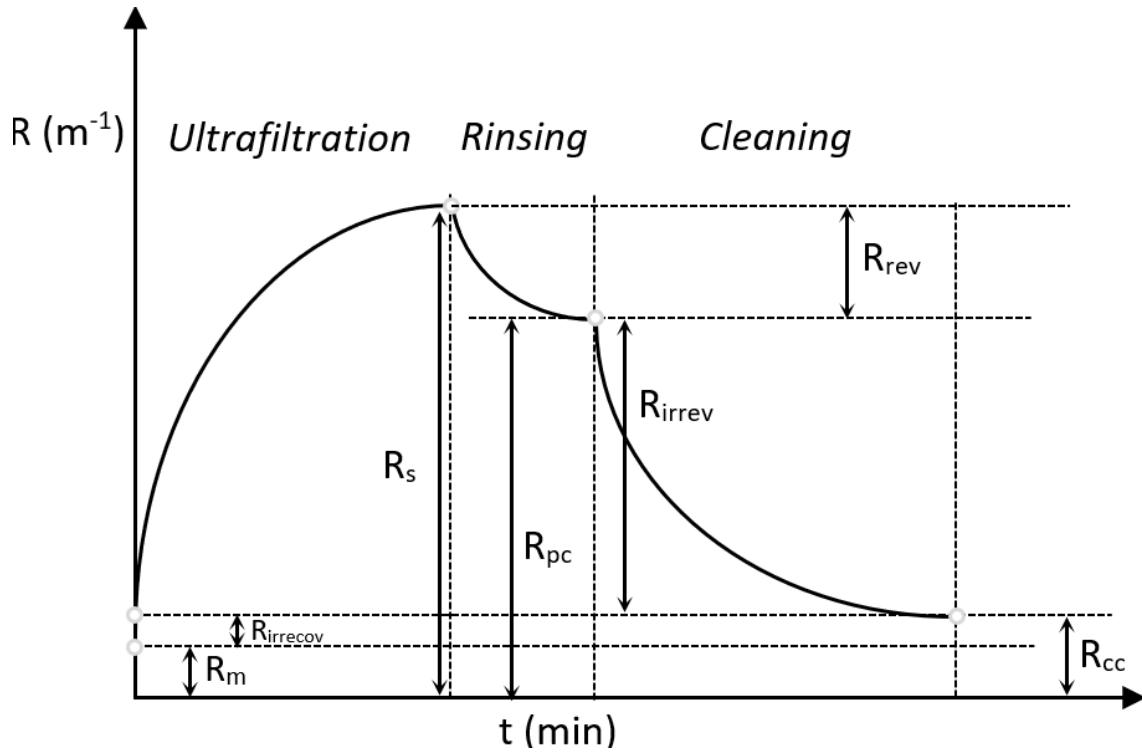
710 Where R_s is total resistance after operation, R_m is the intrinsic membrane resistance,
 711 R_{rev} is the resistance corresponding to reversible fouling, R_{irrev} is the resistance caused by
 712 irreversible fouling, and $R_{irrecov}$ is the resistance referable to irrecoverable fouling.

713 Through simple operations (eqs. A.2-A.4), we can obtain R_{rev} , R_{irrev} and $R_{irrecov}$ with the
 714 resistances calculated with J_s (R_s), J_o (R_m), J_{pc} (R_{pc}) and J_{cc} (R_{cc}) (Figure A.2) [57].

715
$$R_{rev} = R_s - R_{pc} \quad (A.2)$$

716
$$R_{irrev} = R_{pc} - R_{cc} \quad (A.3)$$

717
$$R_{irrecov} = R_{cc} - R_m \quad (A.4)$$



718

719 **Figure A2.** Evolution of resistances during ultrafiltration, rinsing and cleaning. Adapted
 720 from [51].